

# Trajectory Tracking based on Containment Algorithm Applied to a Formation of Mobile Manipulators

Renato Vizquete, Jackeline Abad Torres and Paulo Leica

*Departamento de Automatización y Control Industrial, Escuela Politécnica Nacional, Quito, Ecuador*

**Keywords:** Multi-robot Formation, Distributed Control, Containment Algorithm, Consensus, Mobile Manipulator.

**Abstract:** This paper presents a distributed control for the formation control of mobile manipulators. We use a mobile manipulator model that can be separated in a kinematic and a dynamic component. For the kinematic component (formation control), we propose a distributed containment algorithm with a smooth function to avoid the chattering phenomenon, which provides control actions applicable in real robots. For the dynamic component, a controller based on the compensation of the dynamic forces and torques is applied. The structure of the formation is given by: a group of virtual leaders, which are used as references and to delimit the physic boundaries, and a group of follower robots. The distribution of the followers is determined by a Laplacian matrix, which is built based on the desired positions of the robots inside the convex hull formed by the virtual leaders. To validate the designed controllers, a simulation of formation and tracking trajectory of 8 mobile manipulators is performed, considering as reference, a sinusoid in each coordinate axis.

## 1 INTRODUCTION

The formation control of robots has acquired significant importance in the last decades because of its civil and military applications including moving objects of big dimensions (Eoh et al., 2011), rescue activities (Liu et al., 2013), military convoys (Maxwell et al., 2013), where it is necessary to use multiple robots in a cooperative manner. In many situations, it is crucial to use formations with an irregular geometry according to the circumstances. For instance, the transportation of objects with irregular shapes and heterogeneous distribution of mass requires the use of multiple mobile manipulators in irregular distributions.

One of the challenges in the control of multiple robots formations is the design of decentralized control schemes that consider the complexity and number of robots (or agents in networks), structure and topology of the formation, information flow among the agents, and robustness of the control scheme. Classically, the coordination of multi robots teams (or networks) in a formation uses a centralized architecture, which requires all the network's information to compute the desired actions by the central control. Meanwhile, in a decentralized coordination scheme, every robot computes the control actions based only on local information

(Johnson et al., 2016). In (De La Cruz and Carelli, 2006; Brandao et al., 2014), diverse centralized control systems were developed for the formation control of mobile robots. Despite the satisfactory results of the centralized control schemes, they are vulnerable to failures in the communication network and the operation areas are limited. Further, the scalability and geometric shapes of the formation are other restrictions, which are usually solved by rebuilding the control system.

Distributed control is one of the most relevant techniques for the formation control due to its robustness and scalability, whose most important feature is the distribution of the control capabilities through the system. In this type of architectures, every robot computes the necessary control actions using only the local information provided by its neighbors, without knowing the state of all the formation. Because the controller uses only local information, it is robust to failures in the communication network, which could be catastrophic in a centralized formation control (Tron et al., 2016). Additionally, a distributed formation control allows adding agents and generating different formations characterized by irregular geometric shapes without redesigning the control structure.

Various distributed control methods for multiple mobile robots have been investigated considering limited communication capacity (Bock et al., 2016),

communication delays (Dai and Liu, 2015; Liu et al., 2016), and noise (Dang et al., 2016). For instance, in (Dai and Liu, 2017) a distributed cooperation control considering time delays and obstacles is considered. During the last decade, formation control has been formulated as *containment control* problem, where robots, considered followers, move into a geometric space formed by other robots, considered leaders.

In (Ren and Cao, 2011) and (Cao et al., 2010), several algorithms for the containment control problem have been investigated. Specifically, (Cao et al., 2010) proposes a distributed containment algorithm for double-integrator dynamics, to drive a group of followers into the convex hull spanned by the leaders without considering a specific location of each follower inside the geometric space. The algorithm uses a PD-like controller and a sign function to generate the control actions. The use of this type of function guarantees that the errors of the system converge to zero, but generates control actions with *chattering*. This phenomenon behaves like a high frequency noise due to the switching action of the control law; consequently, the actuator signal is not appropriate for real robots. To avoid this problem, (Cheng et al., 2016) proposes a containment control of multi-agent systems based on a  $PI^n$  type approach considering polynomial trajectories. In (Shtessel et al., 2014) and (Ouyang et al., 2014), a smooth function that approximates the behavior of the sign function is proposed to solve the problem of chattering. The use of smooth functions eliminates the chattering in the control actions, but generates a ball. These controllers cannot guarantee zero error, but the error is confined inside the ball. Depending on the system conditions and the type of these functions, the boundary of the ball could become negligible, getting acceptable results with control actions applicable in a real system.

This work proposes to combine the use of both, the convex hull and smooth functions, which provide a distributed controller with a smooth control action applicable to real manipulators. Here, a distributed controller is designed for the kinematic component of a mobile manipulator while for the dynamic component of each agent another control law is designed based on the dynamics' compensation. Further, the formation is defined using a graph that represents the interactions among the mobile manipulators. The associated graph's matrices (Adjacency, Laplacian matrix among others) and its properties play an important role in the development of the control laws (Godsil and Royle, 2001), which is typical in these types of network dynamics (Xue and Roy, 2012; Jadbabaie et al., 2013; Olfati-Saber, 2006; Cao et al., 2013). Specifically, (Chen and Li,

2008; Chen and Li, 2006) propose an adaptive neural network to control a formation whose geometric pattern is determined by a relative matrix and the interactions among the agents are modelled through a directed graph. In (Zavlanos and Pappas, 2007), the connectivity of a graph represented by the smallest eigenvalue of the Laplacian matrix associated is used to control the movements of the agents in order to track a leader.

In this paper, we aim to present a distributed control system using a smooth function for a formation of mobile manipulators with three degrees of freedom (3 DOF), considering a dynamic model. The paper is organized as follows. In Section II, we formulate the problem of formation control of mobile manipulators as distributed control problem on a network dynamics. Section III presents the kinematic and dynamic model of a mobile manipulator with 3 DOF used in the simulations. In Section IV, the stability of the system including the distributed control law is proved. Section V shows the simulation results in the formation of eight mobile manipulators.

## 2 PROBLEM FORMULATION

The present work focuses on the problem of trajectory tracking of a mobile manipulators formation. The formation is given by a convex hull and a graph that represents the information interchange among the robots.

A convex hull is the minimum convex set formed by a set of points in the Euclidian plane or space. The use of this geometric space allows to delimit the boundaries of the formation and guarantee the location of the robots inside it. The convex hull is formed generally by the *leaders* of the formation, whose movements define the trajectory. In many cases, the robot teams do not have real leaders, and it is necessary to use virtual leaders as a reference for the *followers*. For example, in (Droge, 2015; Yan et al., 2016), a single virtual leader is used for a formation control, while in (Li et al., 2016), multiple leaders are used as references for the flocking of multi-agent systems.

Formally, we consider a formation of  $n$  agents (mobile manipulators) composed by  $m$  mobile manipulators and  $n - m$  virtual leaders. The communication network among the agents, i.e. mobile manipulators and virtual leaders, is modeled through a directed graph (digraph)  $G$ , with undirected communication patterns among the followers and directed paths from the virtual leaders to the followers. The graph  $G = (V, E)$  is formed by a set of

vertices  $V = \{1, \dots, n\}$  that represents the robots/mobile manipulators of the formation and a set of edges  $E \subseteq \{(i, j) \in V \times V : i \neq j\}$  representing the interactions among the robots. For example, if there is a directed interaction between robot  $i = 1$  and robot  $j = 3$  there is a directed edge  $(i, j) = (1, 3)$  in the digraph  $G$ , as shown in Figure 1. The adjacent matrix  $A = [a_{ij}]$  is defined by  $a_{ij} > 0$  if  $(j, i) \in E$  and  $a_{ij} = 0$  otherwise. We define the Laplacian matrix as  $\mathcal{L} = [\ell_{ij}]$ , where  $\ell_{ij} = \sum_{j=1}^n a_{ij}$  if  $i = j$ , and  $\ell_{ij} = -a_{ij}$  if  $i \neq j$ . The adjacent matrix and the Laplacian matrix are related by the expression  $\mathcal{L} = D - A$ , where  $D = \text{diag}\{d_1, \dots, d_n\}$  and  $d_i = \sum_{j=1}^n a_{ij}$  (see (Bapat, 2014) for details on graphs definitions).

Notice that the first  $n - m$  rows of the Laplacian matrix corresponding to the virtual leaders are zeros since there are not interactions from the followers to the leaders or among the leaders, as observed in Figure 1. Due to the fact that the virtual leaders are the reference of the formation, there must be a path from a virtual leader to every follower of the formation. This means the existence of a *connected directed spanning tree* in the graph of the formation.

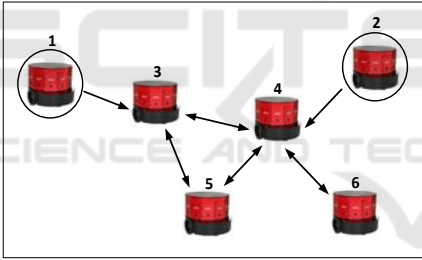


Figure 1: Graph of a communication network among the agents of a formation.

### 3 MOBILE MANIPULATOR

#### 3.1 Kinematic Model

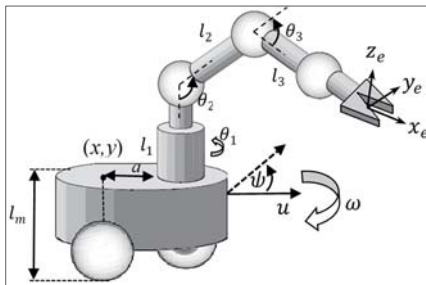


Figure 2: Diagram of a mobile manipulator with 3 DOF (Molina and Suárez, 2016).

A kinematic model of a mobile manipulator with 3 DOF is shown in Figure 2. The effector position of the robot is  $h(t) = [x_e(t) \ y_e(t) \ z_e(t)]^T$ ,  $l_1$ ,  $l_2$  and  $l_3$  are the values of the articulations 1, 2 and 3 respectively,  $\theta_1(t)$ ,  $\theta_2(t)$  and  $\theta_3(t)$  are the angles of the articulations 1, 2 and 3 respectively,  $[x(t) \ y(t)]^T$  is the centroid of the wheels of the manipulator base,  $a$  is the distance from the centroid of the wheels of the mobile platform to the manipulator base,  $l_m$  is the height of the manipulator base;  $u$  and  $\omega$  are the linear and rotational velocities of the platform and  $\psi$  is the orientation of the platform.

The kinematic model of the mobile manipulator is given by:

$$\begin{bmatrix} \dot{x}_e \\ \dot{y}_e \\ \dot{z}_e \end{bmatrix} = J_e \begin{bmatrix} u \\ \omega \\ \dot{\theta}_1 \\ \dot{\theta}_2 \\ \dot{\theta}_3 \end{bmatrix}, \quad (1)$$

where  $J_e$  is the Jacobian matrix of the system defined by:

$$J_e = \begin{bmatrix} J_{11} & J_{12} & J_{13} & J_{14} & J_{15} \\ J_{21} & J_{22} & J_{23} & J_{24} & J_{25} \\ J_{31} & J_{32} & J_{33} & J_{34} & J_{35} \end{bmatrix} \quad (2)$$

$$J_{11} = C_\psi;$$

$$J_{12} = -a S_\psi - S_{\theta_1 \psi} [l_2 C_{\theta_2} + l_3 C_{\theta_2 \theta_3}];$$

$$J_{13} = -S_{\theta_1 \psi} [l_2 C_{\theta_2} + l_3 C_{\theta_2 \theta_3}];$$

$$J_{14} = -C_{\theta_1 \psi} [l_2 S_{\theta_2} + l_3 S_{\theta_2 \theta_3}];$$

$$J_{15} = -l_3 C_{\theta_1 \psi} S_{\theta_2 \theta_3};$$

$$J_{21} = S_\psi;$$

$$J_{22} = a C_\psi + C_{\theta_1 \psi} [l_2 C_{\theta_2} + l_3 C_{\theta_2 \theta_3}];$$

$$J_{23} = C_{\theta_1 \psi} [l_2 C_{\theta_2} + l_3 C_{\theta_2 \theta_3}];$$

$$J_{24} = -S_{\theta_1 \psi} [l_2 S_{\theta_2} + l_3 S_{\theta_2 \theta_3}];$$

$$J_{25} = -l_3 S_{\theta_1 \psi} S_{\theta_2 \theta_3};$$

$$J_{31} = J_{32} = J_{33} = 0;$$

$$J_{34} = l_2 C_{\theta_2} + l_3 C_{\theta_2 \theta_3};$$

$$J_{35} = l_3 C_{\theta_2 \theta_3}$$

where  $C_\psi = \cos\psi$ ;  $S_\psi = \sin\psi$ ;  $S_{\theta_1 \psi} = \sin(\theta_1 + \psi)$ ;  $C_{\theta_2} = \cos\theta_2$ ;  $C_{\theta_2 \theta_3} = \cos(\theta_2 + \theta_3)$ ;  $C_{\theta_1 \psi} = \cos(\theta_1 + \psi)$ ;  $S_{\theta_2} = \sin\theta_2$ ;  $S_{\theta_2 \theta_3} = \sin(\theta_2 + \theta_3)$ .

#### 3.2 Dynamic Model

For the dynamic model, we have considered only the dynamic component of the mobile platform because in most of the mobile manipulators, the weight of the manipulator arm is negligible compared to the

platform and hence the dynamic forces of the arm are also negligible. Also, the rotational velocities of the arm are not considerable compared to other dynamics effects. The dynamic model of the mobile platform is given by:

$$\dot{v} = E + Fv_{ref}, \quad (3)$$

where

$$E = \begin{bmatrix} \frac{\phi_3}{\phi_1}\omega^2 - \frac{\phi_4}{\phi_1}u \\ -\frac{\phi_5}{\phi_2}u\omega - \frac{\phi_6}{\phi_2}\omega \end{bmatrix}, \quad F = \begin{bmatrix} \frac{1}{\phi_1} & 0 \\ 0 & \frac{1}{\phi_2} \end{bmatrix},$$

$$v = \begin{bmatrix} u \\ \omega \end{bmatrix}, \quad v_{ref} = \begin{bmatrix} u_{ref} \\ \omega_{ref} \end{bmatrix},$$

$\phi_1, \phi_2, \phi_3, \phi_4, \phi_5, \phi_6$  are the model parameters, and  $v_{ref}$  is the input vector to the model. The values of these parameters have been chosen for a unicycle robot, according to (De la Cruz, 2006).

Combining the kinematic and dynamic model, the complete model of the mobile manipulator can be expressed as:

$$\begin{bmatrix} \dot{x}_e \\ \dot{y}_e \\ \dot{z}_e \\ \dot{\psi} \\ \dot{u} \\ \dot{\omega} \end{bmatrix} = \begin{bmatrix} J_{11}u + J_{12}\omega \\ J_{21}u + J_{22}\omega \\ J_{31}u + J_{32}\omega \\ \omega \\ \frac{\phi_3}{\phi_1}\omega^2 - \frac{\phi_4}{\phi_1}u \\ -\frac{\phi_5}{\phi_2}u\omega - \frac{\phi_6}{\phi_2}\omega \end{bmatrix} + \begin{bmatrix} 0 & 0 & J_{13} & J_{14} & J_{15} \\ 0 & 0 & J_{23} & J_{24} & J_{25} \\ 0 & 0 & J_{33} & J_{34} & J_{35} \\ 0 & 0 & 0 & 0 & 0 \\ \frac{1}{\phi_1} & 0 & 0 & 0 & 0 \\ 0 & \frac{1}{\phi_2} & 0 & 0 & 0 \end{bmatrix} \begin{bmatrix} u_{ref} \\ \omega_{ref} \\ \dot{\theta}_1 \\ \dot{\theta}_2 \\ \dot{\theta}_3 \end{bmatrix} \quad (4)$$

## 4 CONTROL SYSTEM

### 4.1 Distributed Containment Control

We have chosen a distributed containment control for a double-integrator dynamics:

$$\dot{x}_i(t) = v_i(t), \quad \dot{v}_i(t) = u_i(t), \quad (5)$$

$$i = 1, \dots, n,$$

where  $x_i$ ,  $v_i$ , and  $u_i$  represent position, velocity, and acceleration respectively.

We have used the algorithm for multiple leaders with nonidentical velocities specified in (Cao et al., 2010). In this case, we have selected the sigmoid function for the slide surface  $\gamma\mathcal{L}X + \mathcal{L}\dot{X}$ . Thus, we propose the following algorithm:

$$\ddot{X} = -\mathcal{L}X - \alpha\mathcal{L}\dot{X} - \beta\text{sigm}(\gamma\mathcal{L}X + \mathcal{L}\dot{X}) + \Psi, \quad (6)$$

where  $\text{sigm}(X) = \begin{bmatrix} \frac{x_1}{|x_1|+\varepsilon} & \dots & \frac{x_n}{|x_n|+\varepsilon} \end{bmatrix}^T$ ,  $X = [x_1, \dots, x_n]^T$ ,  $\Psi = [\psi_1, \dots, \psi_n]^T$  is the vector of accelerations with the last  $m$  entries equal to zero and  $\alpha, \beta, \gamma$  and  $\varepsilon$  are positive constants.

Considering  $\tilde{X} \triangleq \mathcal{L}X$ , the state error for the consensus condition, the closed-loop system is given by:

$$\ddot{\tilde{X}} = -\mathcal{L}\tilde{X} - \alpha\mathcal{L}\dot{\tilde{X}} - \beta\mathcal{L}\text{sigm}(\gamma\tilde{X} + \dot{\tilde{X}}) + \mathcal{L}\Psi$$

If we consider only the last  $m$  entries of the system, we get:

$$\ddot{\tilde{X}}_F = -M\tilde{X}_F - \alpha M\dot{\tilde{X}}_F - \beta M\text{sigm}(\gamma\tilde{X}_F + \dot{\tilde{X}}_F) + \Psi_F, \quad (7)$$

where  $\tilde{X}_F$  and  $\Psi_F$  are the vectors containing only the last  $m$  entries and  $M = [m_{ij}] \in \mathbb{R}^{m \times m}$  with  $m_{ij} = \ell_{ij}$ ,  $i, j = n - m + 1, \dots, n$ .

**Remark:** According to the problem formulation,  $M$  is a symmetric matrix with real coefficients. Further, this matrix is diagonally dominant with positive eigenvalues (Gershgorin's circle theorem) (Godsil and Royle, 2001).

In order to prove the system's stability, let us introduce the following matrices:

$$P = \begin{bmatrix} I_m & \gamma M^{-1} \\ \gamma M^{-1} & M^{-1} \end{bmatrix} \quad (8)$$

$$Q = \begin{bmatrix} \gamma I_m & \frac{\alpha\gamma}{2} I_m \\ \frac{\alpha\gamma}{2} I_m & \alpha I_m - \gamma M^{-1} \end{bmatrix} \quad (9)$$

According to (Cao et al., 2010), these matrices are symmetric positive definite if:

$$\gamma < \min \left\{ \sqrt{\lambda_{\min}(M)}, \frac{4\alpha\lambda_{\min}(M)}{4+\alpha^2\lambda_{\min}(M)} \right\},$$

where  $\lambda_{\min}(M)$  represents the minimum eigenvalue of the matrix  $M$ .

We use the Lyapunov function candidate:

$$V = \frac{1}{2} \begin{bmatrix} \tilde{X}_F^T & \dot{\tilde{X}}_F^T \end{bmatrix} P \begin{bmatrix} \tilde{X}_F \\ \dot{\tilde{X}}_F \end{bmatrix}$$

$$V = \frac{1}{2} \tilde{X}_F^T \tilde{X}_F + \gamma \tilde{X}_F^T M^{-1} \dot{\tilde{X}}_F + \frac{1}{2} \dot{\tilde{X}}_F^T M^{-1} \dot{\tilde{X}}_F \quad (10)$$

Deriving (10), we obtain:

$$\begin{aligned} \dot{V} &= \dot{\tilde{X}}_F^T \tilde{X}_F + \gamma \dot{\tilde{X}}_F^T M^{-1} \dot{\tilde{X}}_F + \gamma \tilde{X}_F^T M^{-1} \ddot{\tilde{X}}_F \\ &\quad + \dot{\tilde{X}}_F^T M^{-1} \ddot{\tilde{X}}_F \\ \dot{V} &= -[\tilde{X}_F^T \quad \dot{\tilde{X}}_F^T] Q \begin{bmatrix} \tilde{X}_F \\ \dot{\tilde{X}}_F \end{bmatrix} \\ &\quad - (\gamma \tilde{X}_F^T + \dot{\tilde{X}}_F^T) (-\tilde{X}_F - \alpha \dot{\tilde{X}}_F - M^{-1} \ddot{\tilde{X}}_F) \end{aligned} \quad (11)$$

Then, by applying (7) in (11), the derivative of the Lyapunov candidate is:

$$\begin{aligned} \dot{V} &= -[\tilde{X}_F^T \quad \dot{\tilde{X}}_F^T] Q \begin{bmatrix} \tilde{X}_F \\ \dot{\tilde{X}}_F \end{bmatrix} + (\gamma \tilde{X}_F + \dot{\tilde{X}}_F)^T (M^{-1} \Psi_F) \\ &\quad - \beta (\gamma \tilde{X}_F + \dot{\tilde{X}}_F)^T \text{sigm}(\gamma \tilde{X}_F + \dot{\tilde{X}}_F) \end{aligned} \quad (12)$$

The product  $(\gamma \tilde{X}_F + \dot{\tilde{X}}_F)^T \text{sigm}(\gamma \tilde{X}_F + \dot{\tilde{X}}_F)$  is equivalent to:

$$\begin{aligned} (\gamma \tilde{X}_F + \dot{\tilde{X}}_F)^T \text{sigm}(\gamma \tilde{X}_F + \dot{\tilde{X}}_F) &= \\ &\quad \left\| \gamma \tilde{X}_F + \dot{\tilde{X}}_F \right\|_1 - m\varepsilon \\ &\quad + \sum_{k=1}^m \frac{\varepsilon^2}{\left| (\gamma \tilde{X}_F + \dot{\tilde{X}}_F)_k \right| + \varepsilon} \end{aligned}$$

If  $0 < c < 1$ , the following inequality is satisfied when  $\left\| \gamma \tilde{X}_F + \dot{\tilde{X}}_F \right\|_1 > m\varepsilon/c$ :

$$\begin{aligned} (\gamma \tilde{X}_F + \dot{\tilde{X}}_F)^T \text{sigm}(\gamma \tilde{X}_F + \dot{\tilde{X}}_F) &> \\ &\quad (1-c) \left\| \gamma \tilde{X}_F + \dot{\tilde{X}}_F \right\|_1 \end{aligned}$$

Thus, (12) can be expressed as:

$$\begin{aligned} \dot{V} &< -[\tilde{X}_F^T \quad \dot{\tilde{X}}_F^T] Q \begin{bmatrix} \tilde{X}_F \\ \dot{\tilde{X}}_F \end{bmatrix} + (\gamma \tilde{X}_F + \dot{\tilde{X}}_F)^T (M^{-1} \Psi_F) \\ &\quad - \beta \left[ (1-c) \left\| \gamma \tilde{X}_F + \dot{\tilde{X}}_F \right\|_1 \right] \end{aligned} \quad (13)$$

Using Hölder's inequality and the property of the vector norms  $\|X\|_2 \leq \|X\|_1$  we get:

$$\begin{aligned} (\gamma \tilde{X}_F + \dot{\tilde{X}}_F)^T (M^{-1} \Psi_F) &\leq \left\| \gamma \tilde{X}_F + \dot{\tilde{X}}_F \right\|_2 \|M^{-1} \Psi_F\|_2 \\ &\leq \left\| \gamma \tilde{X}_F + \dot{\tilde{X}}_F \right\|_1 \|M^{-1} \Psi_F\|_1 \end{aligned} \quad (14)$$

Finally, applying (14) in (13), the following inequality is obtained:

$$\begin{aligned} \dot{V} &< -[\tilde{X}_F^T \quad \dot{\tilde{X}}_F^T] Q \begin{bmatrix} \tilde{X}_F \\ \dot{\tilde{X}}_F \end{bmatrix} \\ &\quad - \left\| \gamma \tilde{X}_F + \dot{\tilde{X}}_F \right\|_1 [\beta(1-c) - \|M^{-1} \Psi_F\|_1] \end{aligned}$$

To guarantee  $\dot{V} < 0$ , the following condition must be satisfied:

$$\beta > \frac{\|M^{-1} \Psi_F\|_1}{1-c}$$

Consequently, the system is stable and the errors  $\left\| \gamma \tilde{X}_F + \dot{\tilde{X}}_F \right\|_1$  are limited to a ball with a boundary  $m\varepsilon/c$ . The size of the ball depends on the number of followers  $m$ , the size of the window of the sigmoid function  $\varepsilon$  and a constant  $c \in ]0,1[$ .

## 4.2 Dynamic Controller

The following dynamic controller is proposed:

$$\begin{aligned} v_{ref} &= F^{-1} \chi - F^{-1} E \\ \chi &= \dot{v}_c + \Delta \text{sigm}(\tilde{v}) \\ \Delta &= \begin{bmatrix} \delta_1 & 0 \\ 0 & \delta_2 \end{bmatrix}, \end{aligned} \quad (15)$$

where  $\delta_1$  and  $\delta_2$  are positive constants. To prove stability, the following Lyapunov function candidate is used:

$$V = \frac{1}{2} \tilde{v}^T \tilde{v},$$

where  $\tilde{v} = v_c - v$ , and  $v_c$  is the reference generated by the kinematic (distributed) controller. Taking derivative of  $V$ , we obtain:

$$\dot{V} = \tilde{v}^T \dot{\tilde{v}}$$

$$\dot{\tilde{v}} = -\Delta \text{sigm}(\tilde{v})$$

$$\dot{V} = -\tilde{v}^T \Delta \text{sigm}(\tilde{v})$$

$$\dot{V} = -[\tilde{u} \quad \tilde{\omega}] \begin{bmatrix} \delta_1 & 0 \\ 0 & \delta_2 \end{bmatrix} \begin{bmatrix} \text{sigm}(\tilde{u}) \\ \text{sigm}(\tilde{\omega}) \end{bmatrix}$$

$$\dot{V} = -\delta_1 \tilde{u} \text{sigm}(\tilde{u}) - \delta_2 \tilde{\omega} \text{sigm}(\tilde{\omega})$$

Therefore,  $\dot{V} < 0$ , and hence the system dynamics is stable.

Applying the distributed containment algorithm and the dynamic controller, the complete control system of the formation tracking for each follower is shown in Figure 3. In this figure,  $F_i$ , for  $i = 1, \dots, p$ , represent the neighbors of this follower, i.e. the ones that interact with the follower according to the Laplacian matrix, and  $x_{e_{lj}}, y_{e_{lj}}, z_{e_{lj}}$ , for  $j = 1, \dots, n - m$ , are the states of the virtual leaders.

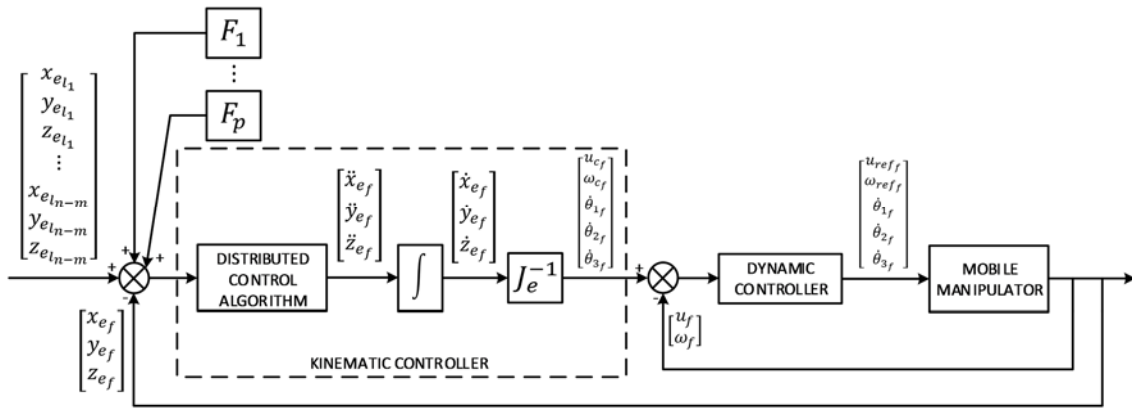


Figure 3: Control system of a follower of the formation.

## 5 SIMULATION

To validate the designed controllers, a simulation has been performed, considering a mobile manipulator with the following dimensions:  $a = 0.2$ ,  $l_1 = 0.383$ ,  $l_2 = 0.233$  and  $l_3 = 0.203$ .

The linear and rotational velocities of the mobile platform are bounded according to the limits of the robot Pioneer 3-DX specified in the datasheet and used in (Yan et al., 2015) ( $-1.2 \leq u \leq 1.2$  (m/s) and  $-5.24 \leq \omega \leq 5.24$  (rad/s)).

The formation uses 12 robots: 8 *real* followers and 4 *virtual* leaders. The positions of the virtual leaders are given by a square inscribed in a circle with radius 3 (m). Additionally, the states of the virtual leaders are determined by the trajectory used as reference. The desired positions of the followers are specified in Table 1.

Table 1: Desired positions of the followers.

Follower	$x(m)$	$y(m)$
$F_1$	0.0	1.75
$F_2$	-1.5	1.0
$F_3$	-1.0	-1.25
$F_4$	1.0	-1.25
$F_5$	1.5	1.0
$F_6$	-0.5	0.5
$F_7$	0.5	0.5
$F_8$	0.0	-0.5

Figure 4 shows the formation of the mobile manipulators, the convex hull spanned by the virtual leaders and the distribution of the followers in it.

Figure 5 shows the graph associated with the formation, which determines the references of each follower.

To find the Laplacian matrix associated with the formation, specifically the weights of the directed edges in the graph, the following system of linear equations is solved:

$$\begin{aligned} \mathcal{L}\mathcal{X} &= 0 \\ \mathcal{L}\mathcal{Y} &= 0 \end{aligned}$$

where  $\mathcal{X}$  and  $\mathcal{Y}$  are the vectors containing the desired positions of the virtual leaders as well as followers in the formation.

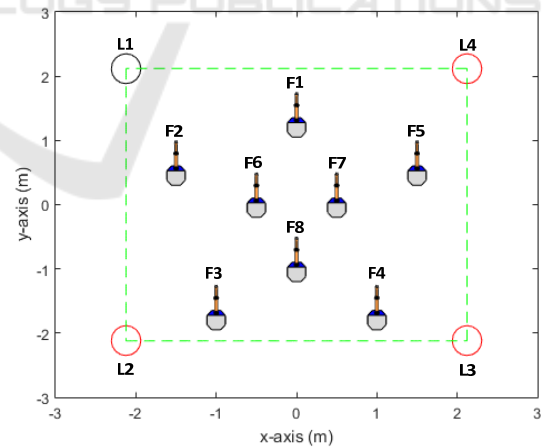


Figure 4: Geometric distribution of the robot formation.

The coefficients of the Laplacian matrix are the unknowns of the system. This is a homogeneous system due to the zeros of the constant terms. For this reason, it is necessary to choose an arbitrary value of one of the coefficients to obtain a nontrivial solution of the system since the robot formation can be formed with an infinite combination of values of the

coefficients of the graph. In this case, the value  $k_4$  is set to 1, which provides the solutions specified in Table 2.

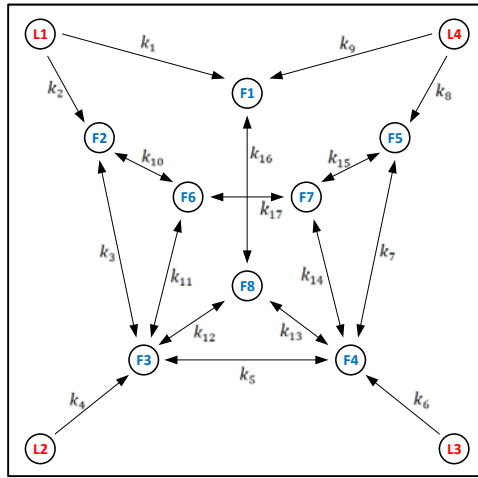


Figure 5: Graph of the formation.

Consequently, the Laplacian matrix of the system is given by:

$$\mathcal{L} = \begin{pmatrix} 0 & 0 & 0 & 0 & 0 & 0 & 0 & 0 & 0 & 0 & 0 & 0 \\ 0 & 0 & 0 & 0 & 0 & 0 & 0 & 0 & 0 & 0 & 0 & 0 \\ 0 & 0 & 0 & 0 & 0 & 0 & 0 & 0 & 0 & 0 & 0 & 0 \\ 0 & 0 & 0 & 0 & 0 & 0 & 0 & 0 & 0 & 0 & 0 & 0 \\ -0.57 & 0 & 0 & -0.57 & 1.33 & 0 & 0 & 0 & 0 & 0 & 0 & -0.19 \\ -0.59 & 0 & 0 & 0 & 0 & 1.07 & -0.24 & 0 & 0 & -0.25 & 0 & 0 \\ 0 & -1 & 0 & 0 & 0 & -0.24 & 2.05 & -0.46 & 0 & -0.07 & 0 & -0.28 \\ 0 & 0 & -1 & 0 & 0 & -0.46 & 2.05 & -0.24 & 0 & -0.07 & -0.28 & 0 \\ 0 & 0 & 0 & -0.59 & 0 & 0 & 0 & -0.24 & 1.07 & 0 & -0.25 & 0 \\ 0 & 0 & 0 & 0 & 0 & -0.25 & -0.07 & 0 & 0 & 0.6 & -0.28 & 0 \\ 0 & 0 & 0 & 0 & 0 & 0 & 0 & -0.07 & -0.25 & -0.28 & 0.6 & 0 \\ 0 & 0 & 0 & 0 & -0.19 & 0 & -0.28 & -0.28 & 0 & 0 & 0 & 0.75 \end{pmatrix}$$

Table 2: Values of the coefficients of the Laplacian matrix.

Edge	Value	Edge	Value	Edge	Value
$k_1$	0.57	$k_7$	0.24	$k_{13}$	0.28
$k_2$	0.59	$k_8$	0.59	$k_{14}$	0.07
$k_3$	0.24	$k_9$	0.57	$k_{15}$	0.25
$k_4$	1	$k_{10}$	0.25	$k_{16}$	0.19
$k_5$	0.46	$k_{11}$	0.07	$k_{17}$	0.28
$k_6$	1	$k_{12}$	0.28		

For the experiment a circular trajectory has been chosen for the  $xy$  plane, while a sinusoid is applied as reference for the vertical movement of the effector in the  $z$ -axis. The equations of the trajectories are:

$$\begin{aligned} x_r &= 4\cos(0.08t) \\ y_r &= 4\sin(0.08t) \\ z_r &= 0.3 + 0.1\sin(0.15t) \end{aligned}$$

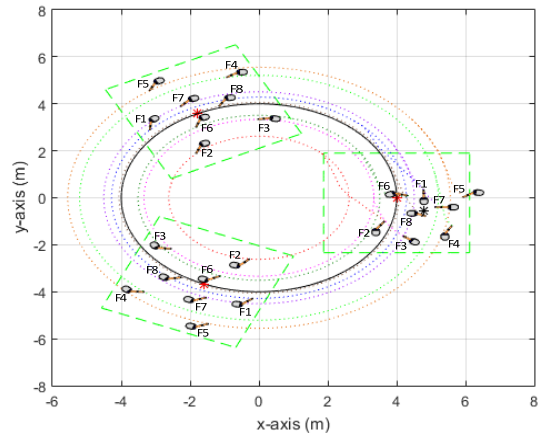


Figure 6: Trajectory of the formation.

The robots start from random positions and achieve the desired positions of the formation quickly. Figure 6 shows the results of the tracking trajectory of the formation in the  $xy$  plane. The movement of the effectors in the  $z$ -axis can be found in Figure 7.

The position errors of the followers' effectors are presented in the Figure 8, Figure 9 and Figure 10. Figure 11 shows the centroid error of the formation. Finally the control actions of the mobile platform are exposed in the Figure 12 and Figure 13. The control actions are smooth and do not present the chattering effect.

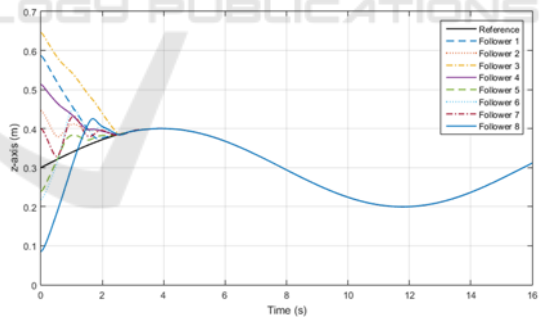


Figure 7: Movement of the effectors in the  $z$ -axis.

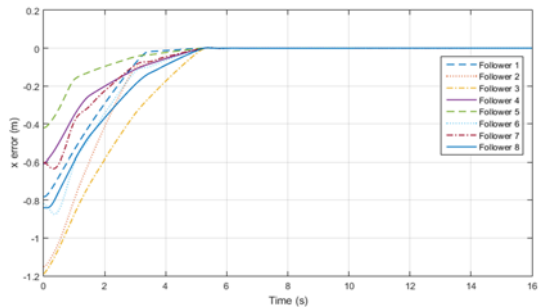


Figure 8:  $x$  error of the followers.

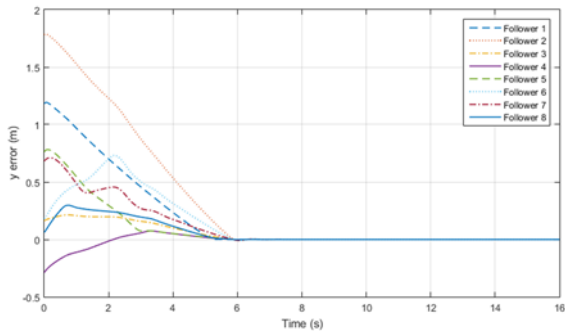


Figure 9: y error of the followers.

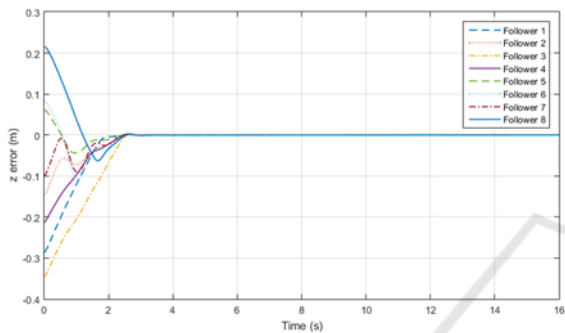


Figure 10: z error of the followers.

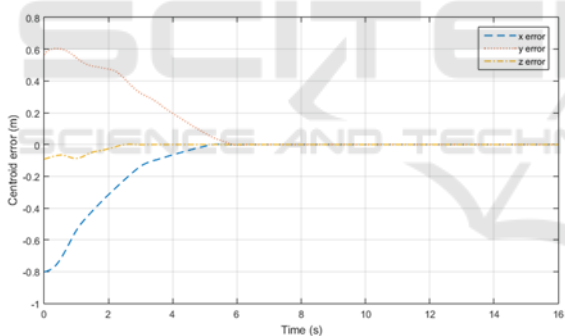


Figure 11: Centroid error of the formation.

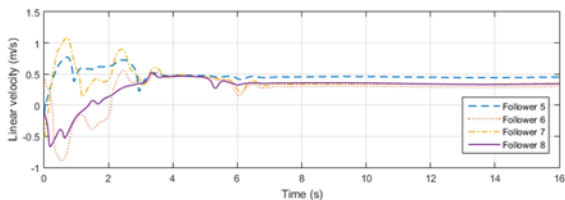
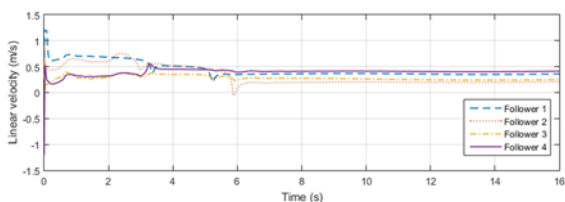


Figure 12: Linear velocity of the followers.

A video of the simulation showing the movements of the robots in the coordinate axes can be found at [https://www.youtube.com/watch?v=bc\\_S9HWAM0gg](https://www.youtube.com/watch?v=bc_S9HWAM0gg)

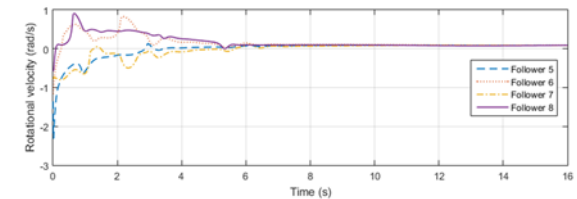
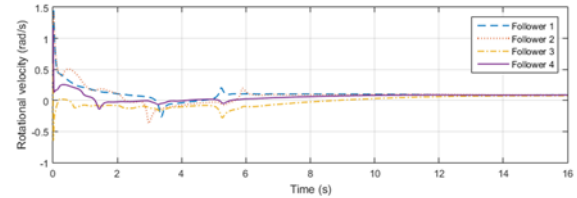


Figure 13: Rotational velocity of the followers.

## 6 CONCLUSIONS

In this paper, we proposed a distributed control for the formation control of mobile manipulators. A distributed containment control was proposed for the kinematic component. A controller based in the compensation of the dynamic forces and torques was proposed for the dynamic component. The two controllers designed were applied using a cascade control architecture. The structure of the formation was given only by the Laplacian matrix, whose coefficients were found solving a system of linear equations obtained by considering the desired positions of the followers inside the convex hull spanned by the virtual leaders.

The virtual leaders were used as references and determined only by the desired trajectory. The control actions obtained did not show the chattering phenomenon and were limited to the values of velocities of a real robot.

## ACKNOWLEDGEMENTS

The authors thanks Escuela Politécnica Nacional for the grant support PII-DACI-01-2017 and PIJ-15-17.

## REFERENCES

Bapat, R. (2014). *Graphs and Matrices*. London: Springer-Verlag.

- Bock, G., Hendrickson, R., Lamkin, J., Dhall, B., Wang, J., and Ahn, I. (2016). Experiments of distributed control for multiple mobile robots with limited sensing/communication capacity. In: *IEEE International Conference on Electro Information Technology (EIT)*. Grand Forks, ND, USA.
- Brandao, A., Barbosa, J., Mendoza, V., Sarcinelli-Filho, M., and Carelli, R. (2014). A Multi-Layer Control Scheme for a centralized UAV formation. In: *International Conference on Unmanned Aircraft Systems (ICUAS)*. Orlando, FL, USA.
- Cao, Y., Stuart, D., Ren, W., and Meng, Z. (2010). Distributed Containment Control for Double-integrator Dynamics: Algorithms and Experiments. In: *American Control Conference (ACC)*. Baltimore, MD, USA.
- Cao, Y., Yu, W., Ren, W., and Chen, G. (2013). An Overview of Recent Progress in the Study of Distributed Multi-Agent Coordination. *IEEE Transactions on Industrial Informatics*, 9(1), 427-438.
- Chen, X., and Li, Y. (2006). Smooth Formation Navigation of Multiple Mobile Robots for Avoiding Moving Obstacles. *International Journal of Control, Automation, and Systems*, 4(4), 466-479.
- Chen, X., and Li, Y. (2008). Stability on Adaptive NN Formation Control with Variant Formation Patterns and Interaction Topologies. *International Journal of Advanced Robotic Systems*, 5(1), 69-82.
- Cheng, L., Wang, Y., Ren, W., Hou, Z.-G., and Tan, M. (2016). Containment Control of Multiagent Systems With Dynamic Leaders Based on a Pin-Type Approach. *IEEE Transactions on Cybernetics*, 46(12), 3004-3017.
- Dai, G.-B., and Liu, Y.-C. (2015). Leaderless and leader-following consensus for networked mobile manipulators with communication delays. In: *IEEE Conference on Control Applications (CCA)*. Sydney, Australia.
- Dai, G.-B., and Liu, Y.-C. (2017). Distributed Coordination and Cooperation Control for Networked Mobile Manipulators. *IEEE Transactions on Industrial Electronics*, 64(6).
- Dang, A., La, H., and Horn, J. (2016). Distributed formation control for autonomous robots following desired shapes in noisy environment. In: *IEEE International Conference on Multisensor Fusion and Integration for Intelligent Systems (MFI)*. Baden, Germany.
- De la Cruz, C. (2006). Control de Formación de Robots Móviles. *Tesis Doctoral, INAUT-UNSJ*.
- De La Cruz, C., and Carelli, R. (2006). Dynamic Modeling and Centralized Formation Control of Mobile Robots. In: *IECON 2006 - 32nd Annual Conference on IEEE Industrial Electronics*. Paris, France.
- Droge, G. (2015). Distributed virtual leader moving formation control using behavior-based MPC. In: *American Control Conference (ACC)*. Chicago, IL, USA.
- Eoh, G., Jeon, J., Choi, J., and Lee, B. (2011). Multi-robot cooperative formation for overweight object transportation. In: *IEEE/SICE International Symposium on System Integration (SII)*. Kyoto, Japan.
- Godsil, C., and Royle, G. (2001). *Algebraic Graph Theory*. New York: Springer-Verlag.
- Jadbabaie, A., Lin, J., and Morse, A. (2003). Coordination of groups of mobile autonomous agents using nearest neighbor rules. *IEEE Transactions on Automatic Control*, 48(6), 988-1001.
- Johnson, L. B., Choi, H. L., and How, J. P. (2016). The Role of Information Assumptions in Decentralized Task Allocation: A Tutorial. *IEEE Control Systems*, 36(4), 45-46.
- Li, Z., Na, C., and Xie, G. (2016). Flocking of Multi-Agent Systems with Multiple Virtual Leaders Based on Connectivity Preservation Approach. In: *Proceedings of the 2015 Chinese Intelligent Systems Conference, Volume 1* (págs. 465-473). Berlin: Springer-Verlag.
- Liu, Y., Nejat, G., and Vilela, J. (2013). Learning to cooperate together: A semi-autonomous control architecture for multi-robot teams in urban search and rescue. *2013 IEEE International Symposium on Safety, Security, and Rescue Robotics (SSRR)*. Linköping, Sweden.
- Liu, Z., Chen, W., Lu, J., Wang, H., and Wang, J. (2016). Formation Control of Mobile Robots Using Distributed Controller With Sampled-Data and Communication Delays. *IEEE Transactions on Control Systems Technology*, 24(6), 2125-2132.
- Maxwell, P., Rykowski, J., and Hurlock, G. (2013). Proposal for the initiation of general and military specific benchmarking of robotic convoys. In: *IEEE Conference on Technologies for Practical Robot Applications (TePRA)*. Woburn, MA, USA.
- Molina, L., and Suárez, J. (2016). *Seguimiento de trayectoria mediante tres estrategias de control basado en espacio nulo, control en modo deslizante (SMC) y tipo PID aplicadas a una formación de manipuladores móviles*. Thesis, Escuela Politécnica Nacional. Quito, Ecuador.
- Olfati-Saber, R. (2006). Flocking for multi-agent dynamic systems: algorithms and theory. *IEEE Transactions on Automatic Control*, 51(3), 401-420.
- Ouyang, P. R., Acob, J., and Pano, V. (2014). PD with sliding mode control for trajectory tracking of robotic system. *Robotics and Computer-Integrated Manufacturing*, 30(2), 189-200.
- Pioneer 3-DX Datasheet, Adept Technology, Inc. Rev. A. <http://www.mobilerobots.com/Libraries/Downloads/Pioneer3DX-P3DX-RevA.sflb.ashx>.
- Ren, W., and Cao, Y. (2011). *Distributed Coordination of Multi-agent Networks*. London: Springer-Verlag.
- Shtessel, Y., Edwards, C., Fridman, L., and Levant, A. (2014). *Sliding Mode Control and Observation*. Basel: Birkhäuser.
- Tron, R., Thomas, J., Loianno, G., Daniilidis, K., and Kumar, V. (2016). A Distributed Optimization Framework for Localization and Formation Control: Applications to Vision-Based Measurements. *IEEE Control Systems*, 36(4), 22-24.
- Xue, M., and Roy, S. (2012). Characterization of security levels for the dynamics of autonomous vehicle networks. In: *IEEE 51st Annual Conference on*

- Decision and Control (CDC)*, (pp. 3916-3921). Maui, HI, USA.
- Yan, Z., Fabresse, L., Laval, J., and Bouraqadi, N. (2015). Metrics for Performance Benchmarking of Multi-robot Exploration. In: *IEEE/RSJ International Conference on Intelligent Robots and Systems (IROS)*. Hamburg, Germany.
- Yan, Z., Liu, X., Jiang, A., and Wang, L. (2016). Formation control of multiple UUVs based on virtual leader. In: *35th Chinese Control Conference (CCC)*. Chengdu, China.
- Zavlanos, M., and Pappas, G. (2007). Potential Fields for Maintaining Connectivity of Mobile Networks. *IEEE Transactions on Robotics*, 23(4), 812-816.

